Interfacial Processes in EES Systems Advanced Diagnostics

Robert Kostecki
Lawrence Berkeley National Laboratory
Berkeley, California 94720

June 17, 2014

Project ID# ES085

Overview

Timeline

- PI participates in the BATT Program since 1999
- This project was recompeted in FY12 and renewed in FY13

Barriers Addressed

- Low Li-ion battery energy density, and calendar/cycle lifetimes for PHV and EV applications
- Inadequate cell/electrode impedance that limits power and affects system safety

Budget

- FY14 funding $500K
- FY13 funding $500K
- FY12 funding $520K

Partners

- BATT Cathode and Anode Task Groups: ANL, LBNL, SUNY, UP, HQ and UG.
- V. Srinivasan, M. Foure (BATT Program management)
- The Northeastern Center for Chemical Energy Storage
- UCSD (D. Basov group)
- LBNL Advanced Light Source

Relevance: Objectives

1. Unveil the structure and reactivity at hidden or buried interfaces and interphases that determine battery performance and failure modes.
   - Obtain detailed insight into the dynamic behavior of molecules, atoms, and electrons at electrode/electrolyte interfaces of intermetallic anodes (Si) and high voltage Ni/Mn-based materials.
2. Establish clear connections between diagnostics, theory/modelling, materials synthesis, and cell development efforts.
   - Provide remedies to interface instability e.g., artificial surface layers (e.g., ALD) and/or structures, novel electrode architecture, electrolyte additives, co-intercalation of secondary metals/ions etc.
   - Characterize active material/electrode/cell degradation modes, improve long-term stability of high-energy Li-ion systems.
3. Develop and deploy novel *in situ* far- and near-field optical multifunctional probes.
   - Achieve spatial and temporal resolution that corresponds to the size and rate of basic chemical steps and structural, building blocks.

Milestones

- Determine the origin of fluorescent species that are produced at high-energy Li-ion cathodes (December, 2013)
    - Accomplished on time. Fluorescence originated from the formation of Ni(II) and Mn(II) coordination complexes with β-keto esters ligands
- Resolve SEI layer chemistry of Si and Sn model single crystal anodes (March, 2014)
    - Accomplished on time. *In situ* studies revealed that the nature and kinetics of surface reactions are strongly dependent on the Si and Sn surface crystal orientation, electrolyte composition and presence of native oxides.
- Characterize interfacial phenomena in high-voltage composite cathodes (June 2014)
    - Work in progress ~ 70% completed. The exact mechanism of electrolyte oxidation and its implications to the cell electrochemical performance are currently being elborated and assessed. Degradation phenomena occurs at the interface by reaction between interfacial atoms and electrolyte decomposition products to form coordination complexes at the cathode surface during oxidation
- Demonstrate feasibility of in situ near-field techniques to study interfacial phenomena at Li-battery electrodes (September 2014)
    - Work in progress ~ 60% completed. Acquired near-field spectroscopic information of the SEI layer for both silicon and tin

Morphology and Topology of Li-cell

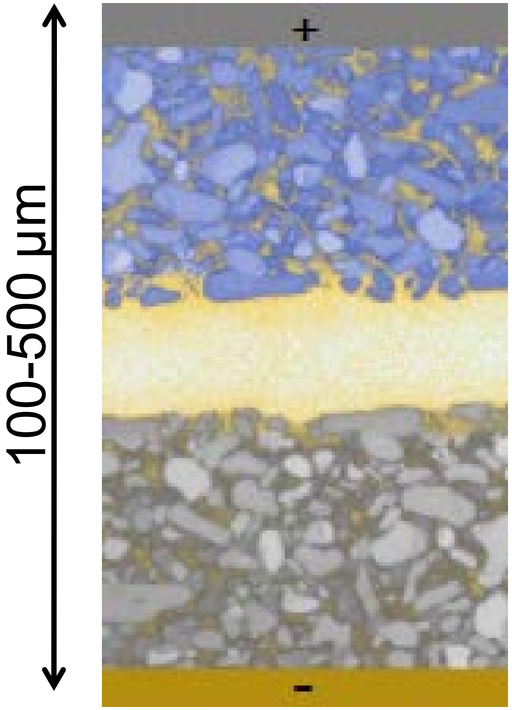

H. Gabrish, UNO

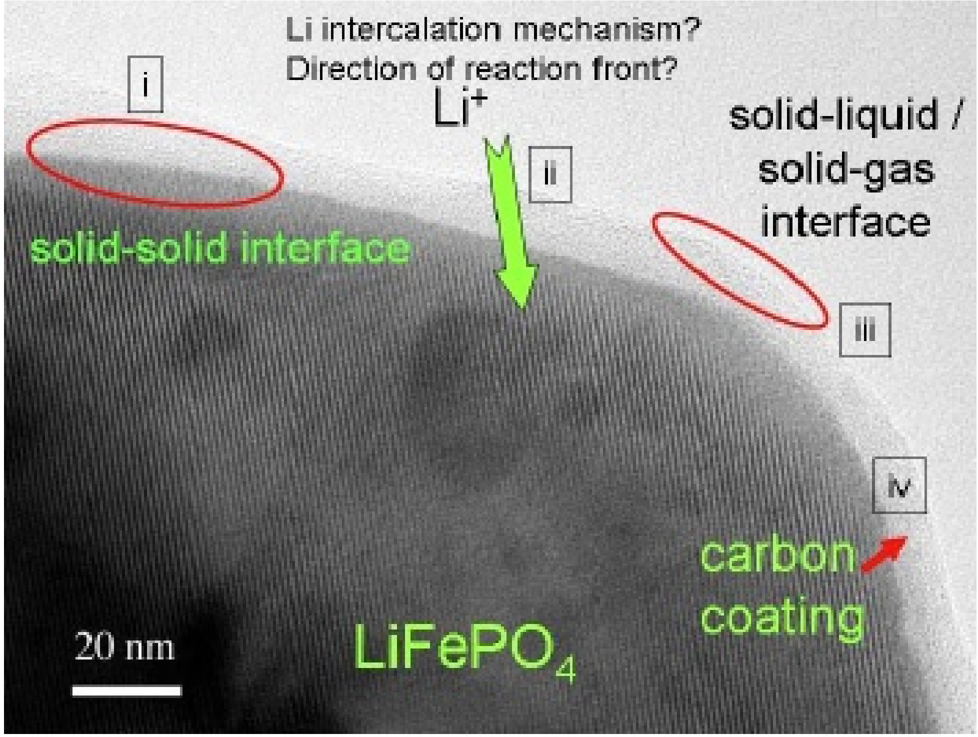

- A battery system involves interactions among various states of matter.
- A simple electrode design must be meticulously optimized for every active material chemistry, particle size, morphology and topology.

The influence of electrode surface structure on electrochemical reaction rates and mechanisms is a major challenge in battery research where electrodes with inherent structural heterogeneities are used ubiquitously

EES Analytical Tools – Basic Parameters

Sensitivity, Selectivity, Specificity

Spatial, Temporal and Energy Resolution

In situ probing/monitoring

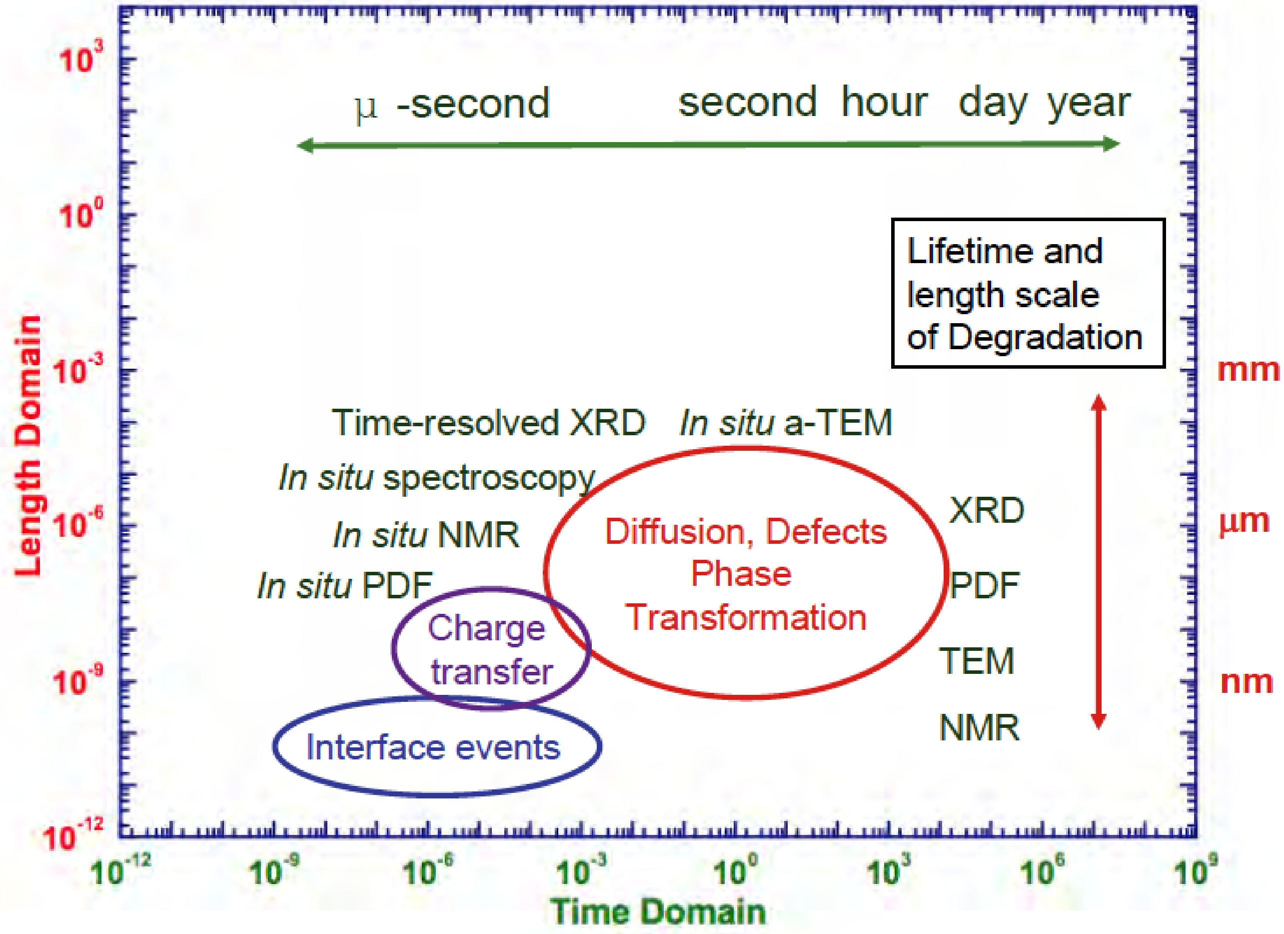

Novel Characterization Strategies for EES Systems

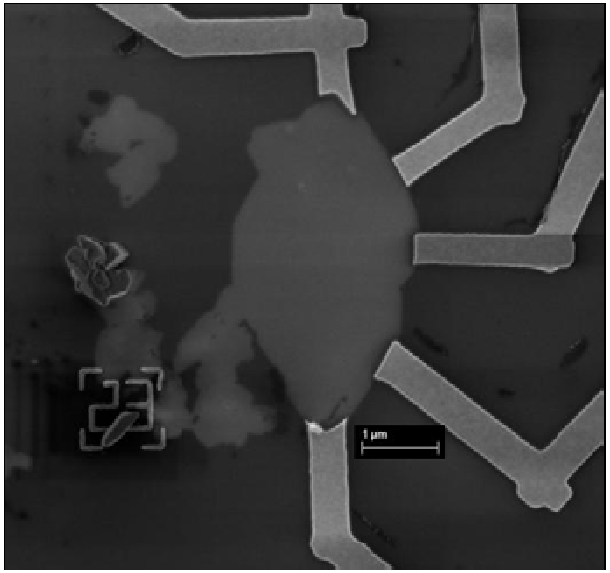

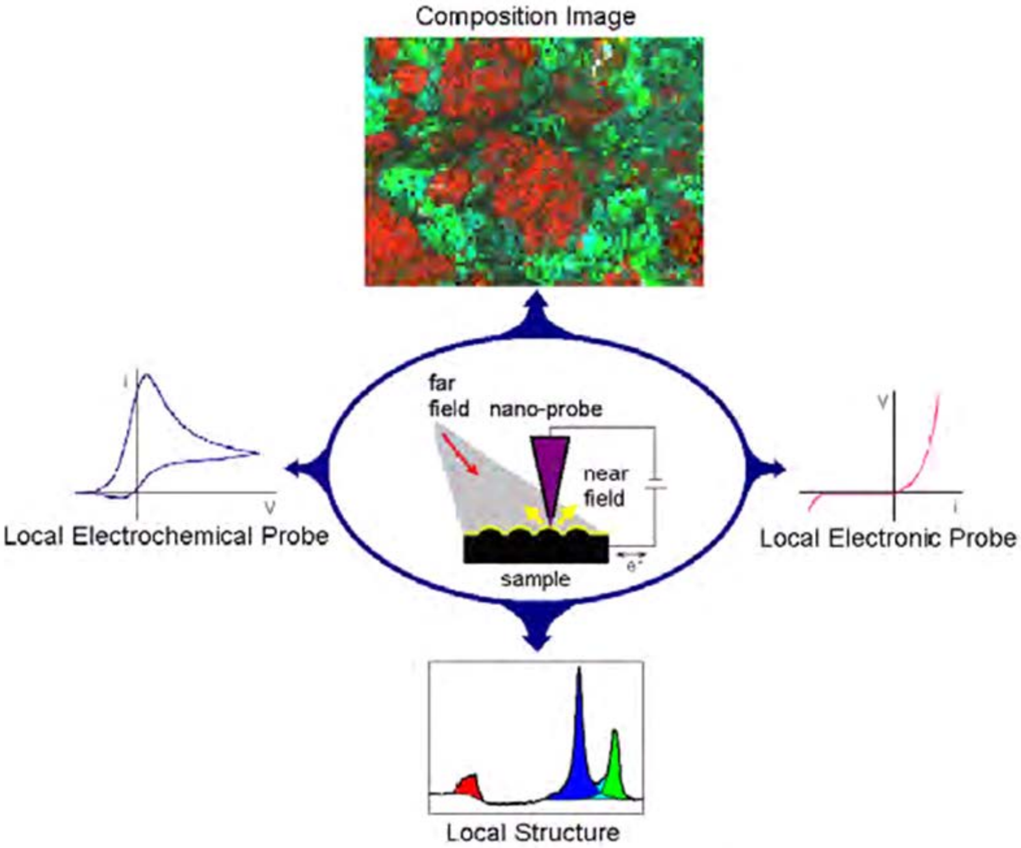

- Design new *ex situ* and *in situ* characterization methodologies to study EES materials and interfaces in a mono-molecular, single micro- and nano-particle configurations.
- Apply them to address key scientific and technology challenges of high-energy Li-ion cells for PHEV and EV applications.

Interfacial Activity of High-Voltages Cathodes

Approach

- Apply *in situ* and *ex situ* Raman, fluorescence, FTIR, X-ray absorption spectroscopy and standard electrochemical techniques to characterize interfacial phenomena on $LiNi_{0.5}Mn_{1.5}O_4$ during charge/discharge
  - Perform *in situ* measurements on composite cathodes and model single particle electrodes
  - Monitor molecular "shuttle" phenomena in Li-ion cells and assess their impact on the cell electrochemical performance

Accomplishments

- Determined the mechanism of interfacial processes on $LiNi_{0.5}Mn_{1.5}O_4$ and chemical cross-talk in high-energy Li-ion cells
  - Mn and/or Ni dissolution leads to formation of Ni(II) and Mn(II) coordination complexes, which diffuse toward the anode and get integrated in the SEI at the graphite surface (SEI Mn/Ni poisoning)
  - Insoluble electrolyte decomposition products form electronic and ionic barriers in composite cathodes and contribute to the impedance rise in graphite anodes in Li-ion cells.

In situ Spectroscopy of $LiNi_{0.5}Mn_{1.5}O_4$ Single Particle Electrodes

Electrochemical response

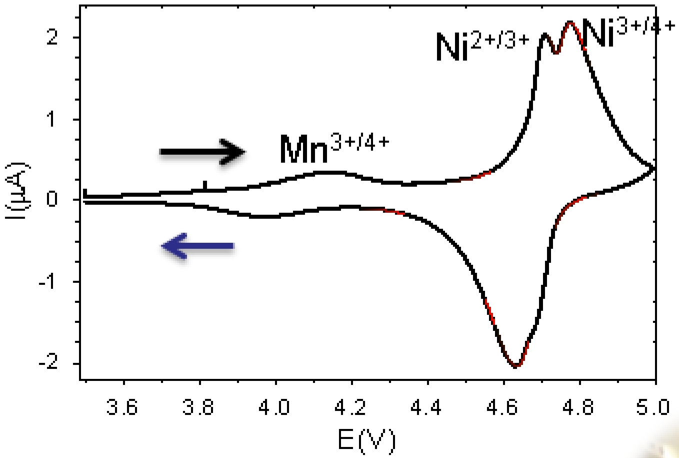

Fluorescence Spectroscopy

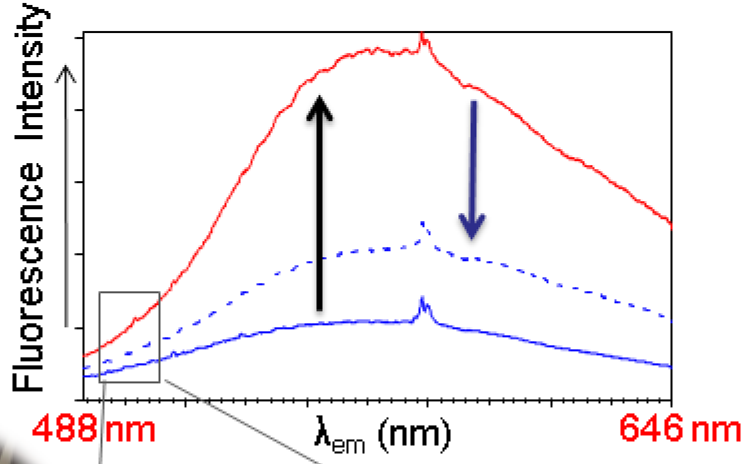

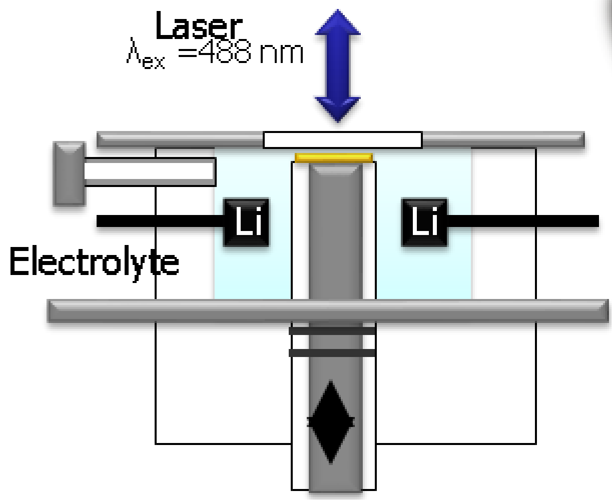

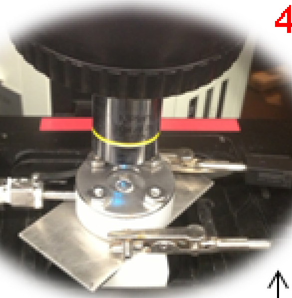

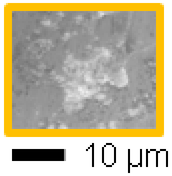

Working electrode
LMNO powder
pressed into Al foil

Raman Spectroscopy

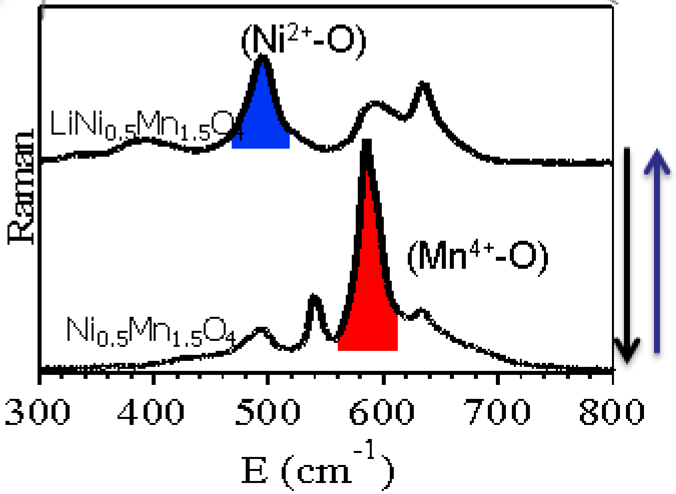

Electrolyte Oxidation at $LiNi_{0.5}Mn_{1.5}O_4$

Strong Fluorescence Signal

$LiNi_{0.5}Mn_{1.5}O_4$ [1]

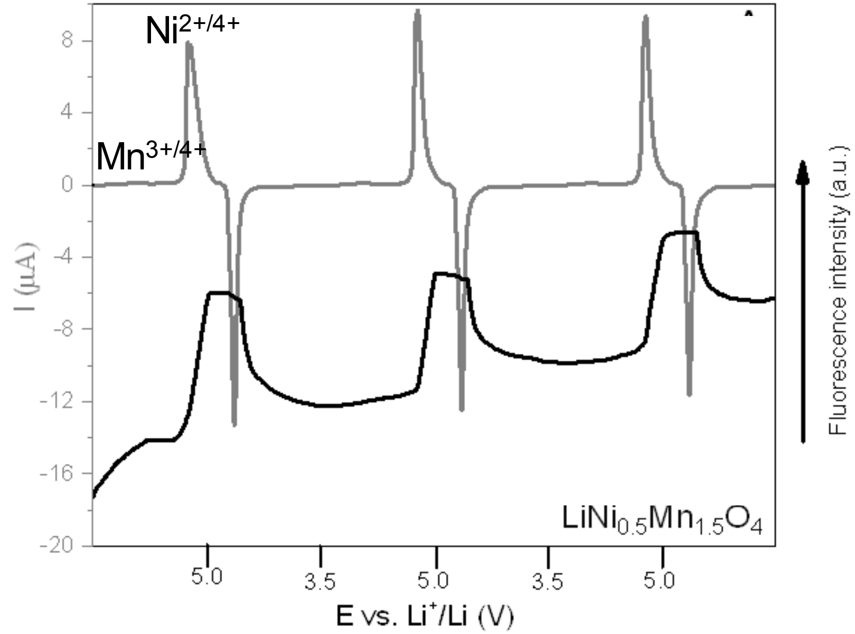

$LiMn_2O_4$

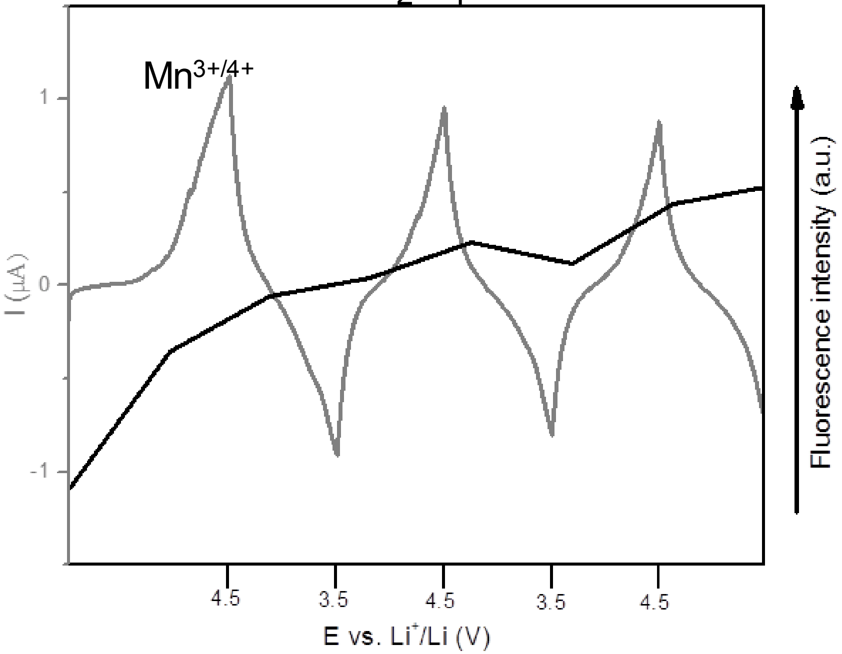

- Fluorescence compounds form during electrolyte oxidation at LNMO. Fluorescence signal rises at the beginning of Ni^{2+} oxidation
- Some fluorescent decomposition products dissolve in the electrolyte whereas other tend to accumulate at the LMNO surface forming a surface thin-film.
- Strong fluorescence is also observed at $LiMn_2O_4$ and in $LiClO_4$-based organic carbonate electrolytes.

[1] Norberg, N. S., Lux, S. F. & Kostecki, R. Electrochemistry Communications 34, 29-32, (2013)

Surface Film at Cycled Composite Cathodes

FTIR

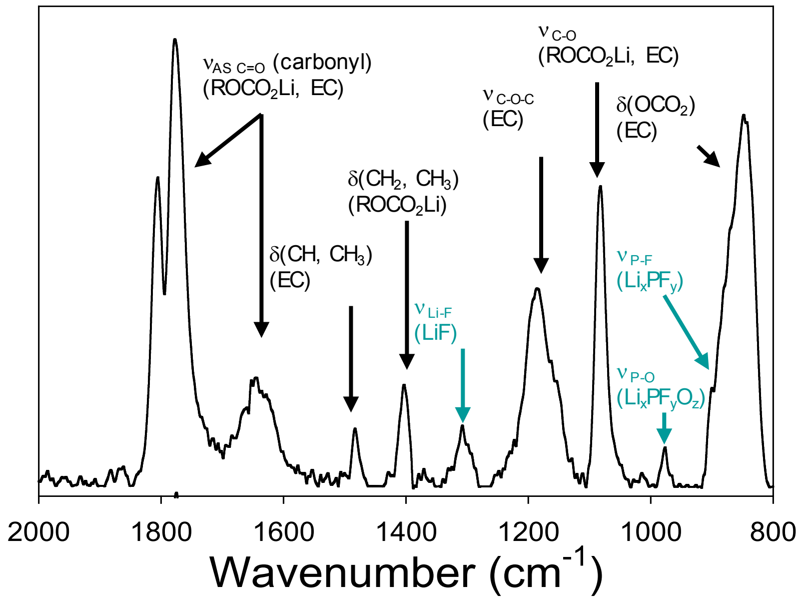

Fluorescence Image

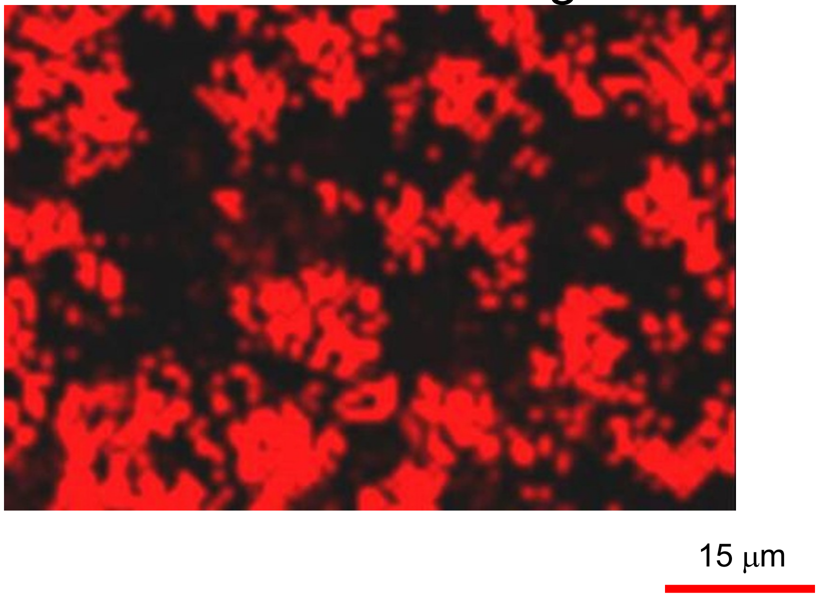

- Surface of tested cathodes exhibits a non-uniform pattern of fluorescing spots
- FTIR spectra reveal the presence of solvent residues (EC), $LiPF_6$ salt and organic electrolyte decomposition products
- Fluorescence compounds originate from the decomposition of organic carbonate electrolytes

Formation of Fluorescent Metal Complexes at the $LiNi_{0.5}Mn_{1.5}O_4$ Surface

$LiNi_{0.5}Mn_{1.5}O_4$ spinel operates at 4.7 V vs. Li^+/Li^0 i.e., well outside the thermodynamic stability window of the electrolyte.

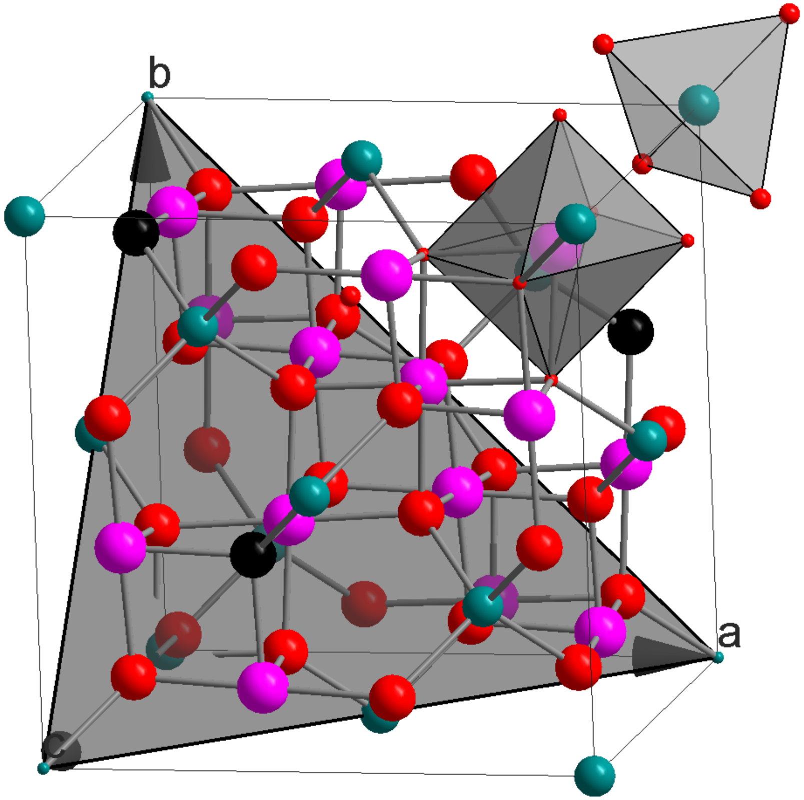

- (111) facet dominates the particle morphology[1-2]
- Presence of oxygen vacancies leads to reduction of manganese at the surface and increases oxygen surface mobility

[1] A. Karim, S. Fosse, K. A. Persson, Physical Review B 2013, 87, 075322.
[2] L. Eunseok, K. Persson, Nanotechnology, 2013, 24, 424007

Reaction Pathways to Fluorescent Metal Complexes I

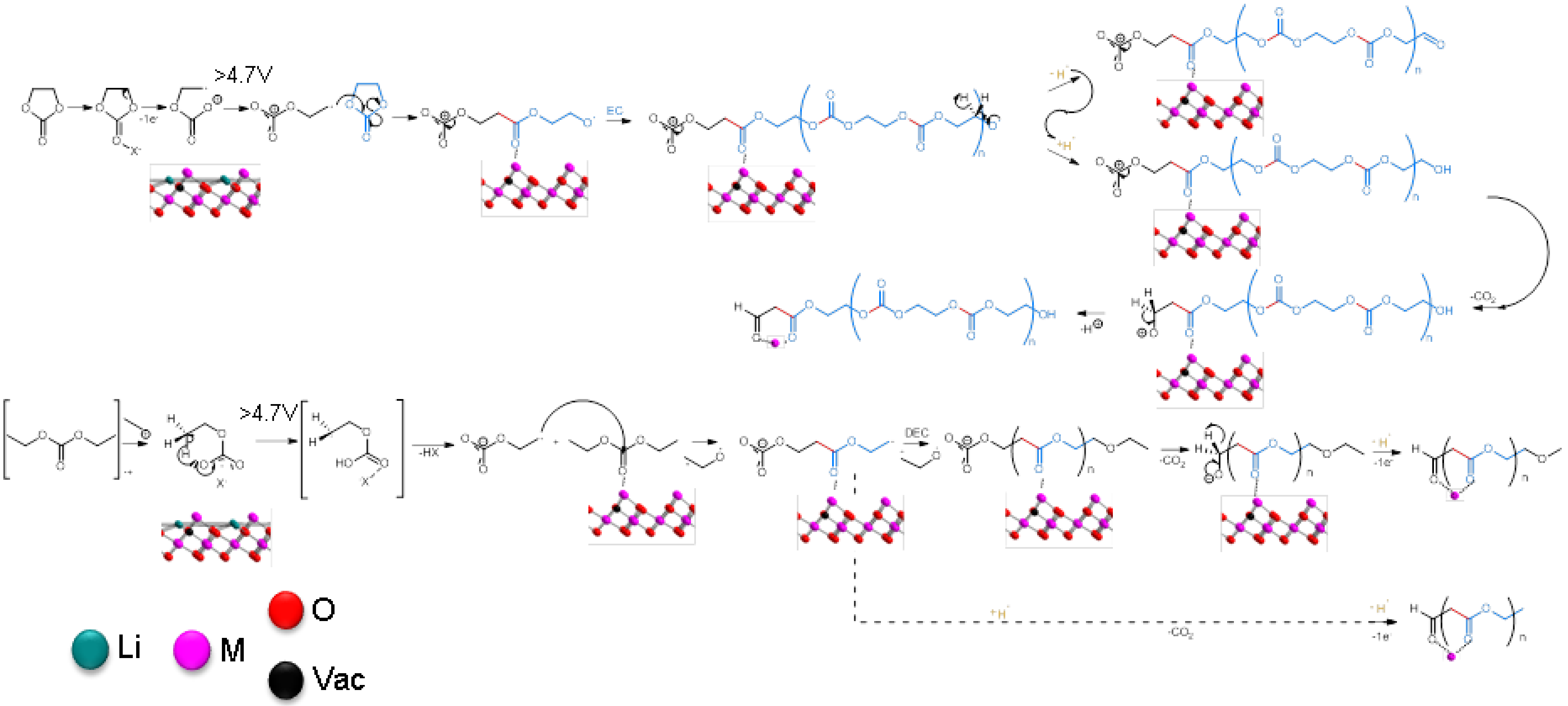

Formation of coordination complexes with β-keto esters ligands at the cathode surface during oxidation leads to CO_2 release.

Reaction Pathways to Fluorescent Metal Complexes II

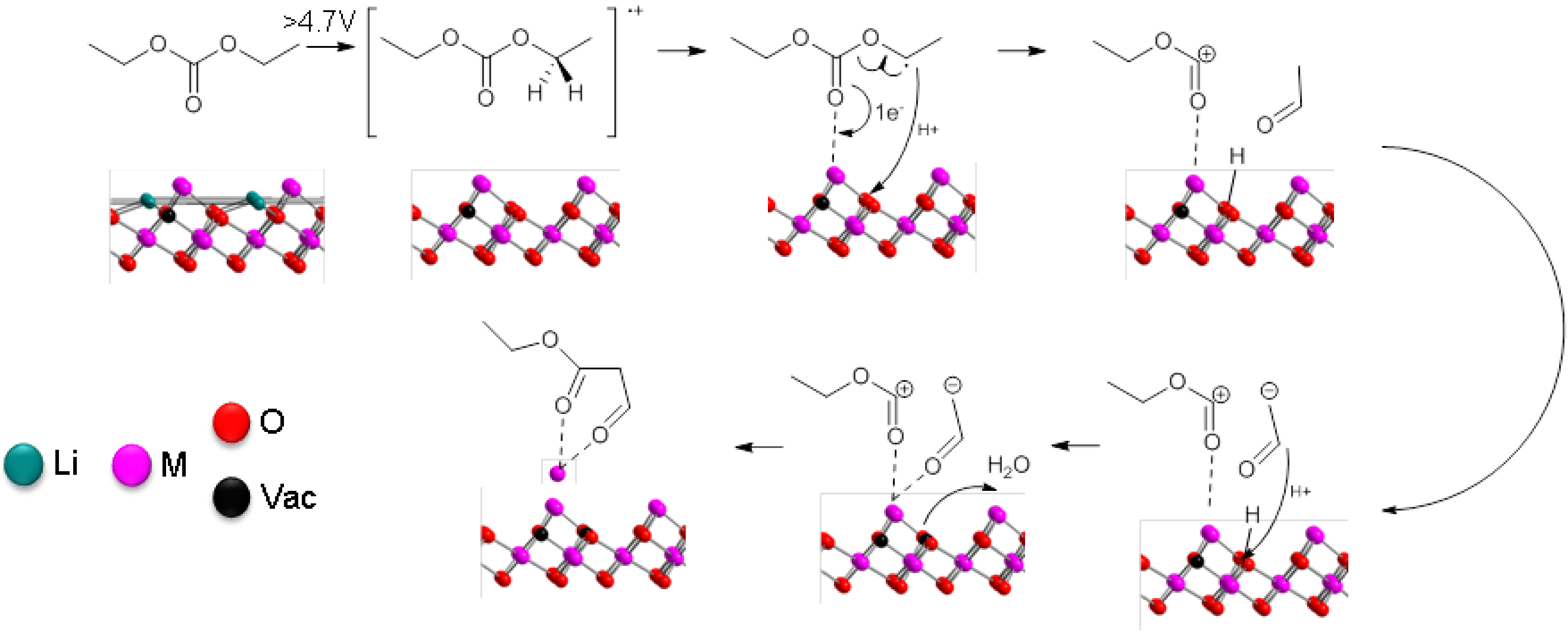

- Formation of coordination complexes with β-keto esters ligands at the cathode surface during oxidation leads to H_2O release
- Presence of oxygen vacancies, O-H and ligands bonds forming at the LMNO surface favors the metal dissolution by weakening the M-O bond strength

Fluorescence Emission from aged $LiNi_{0.5}Mn_{1.5}O_4$ and Graphite Electrodes

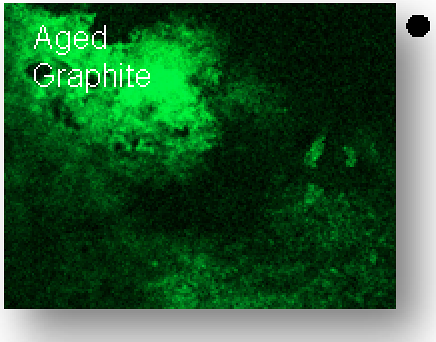

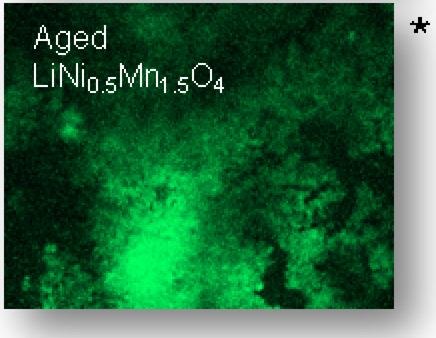

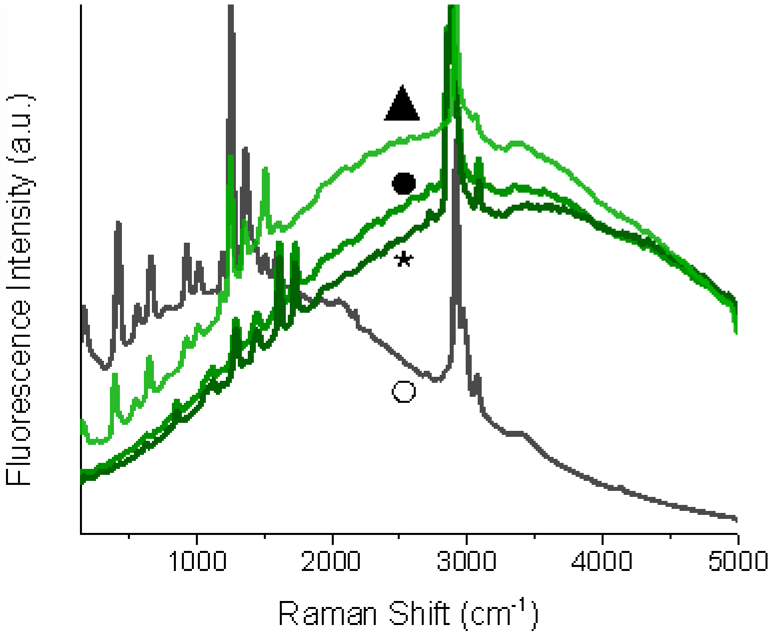

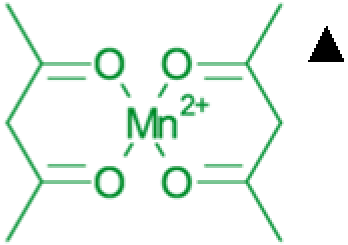

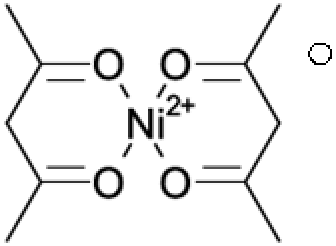

- Surface distribution of fluorescence species and *ex situ* Raman spectra of a graphite anode (∗) and $LiNi_{0.5}Mn_{1.5}O_4$ cathode (●) from a coin cell cycled galvanostatically 600 times shows that the fluorescent species formed originally at the $LiNi_{0.5}Mn_{1.5}O_4$ diffuse/migrate toward the graphite anode and get incorporated into the SEI

- The spectral baseline from the cycled electrode displays a broad and intense fluorescence background which is very similar to that of Mn(II) acetylacetonate indicating the presence of metal complexes with β-keto esters ligands at the surface of the aged cathode and anode

Mn(II)/Ni(II) Complexes in the SEI of Aged Graphite Anode

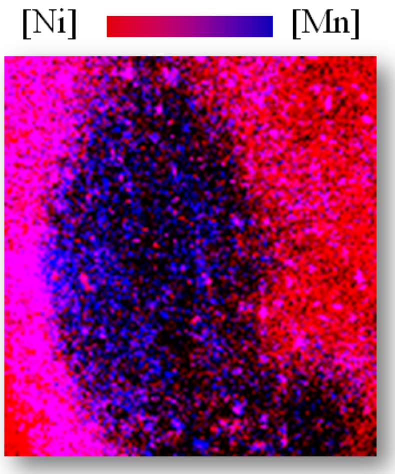

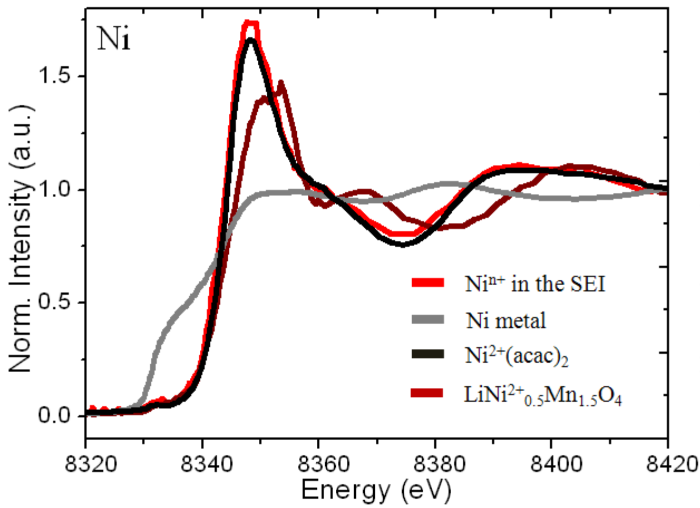

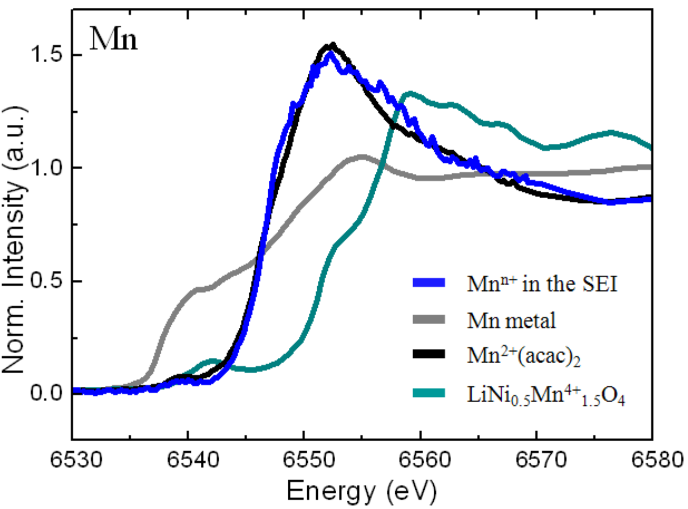

- XANES experiments demonstrated that Mn^{2+} and Ni^{2+} are non-uniformly distributed in the SEI layer suggesting different chemical affinity of fluorescent species to specific compounds in the SEI layer
- The presence of coordination complexes within the SEI similar to metal acetylacetonates, i.e, Ni(II) and Mn(II) coordination complexes with β-keto esters Ligands, is confirmed

Summary I

- LMNO electrode/electrolyte interface exhibits a fluorescence rise correlated with the beginning of the Ni^{2+} (ca. 4.2 V)

- Ni(II) and Mn(II) coordination complexes form at the $LiNi_{0.5}Mn_{1.5}O_4$ surface via reaction between interfacial atoms and the organic carbonate solvents oxidation products

- The Ni(II) and Mn(II) coordination complexes with β-keto esters ligands partially dissolve in the electrolyte, diffuse towards the anode and get integrated in the SEI at the graphite surface
  - The SEI layer formed at the graphite surface contains Ni(II) and Mn(II) not metallic Mn and Ni as proposed in the literature.

The mechanism of the SEI layer "poisoning" by the Ni(II) and Mn(II) coordination complexes remains unclear at this moment but it can be used to study basic functions and operation of SEIs in Li-ion systems.

Sn Negative Electrode for Li-ion Systems

- Large specific capacity (993 $mAhg^{-1}$) vs. graphite (372 $mAhg^{-1}$)
- Fast diffusion of Li in Sn – fast rate anode material

- Large irreversible capacity loss during early cycles and poor reversible capacity retention
- Large volumetric changes upon alloying and dealloying, particle decrepitation, and loss of electronic contact

Solid electrolyte interphase (SEI) determines the irreversible capacity loss, cycle- and calendar lifetime of LIB systems

Fundamental understanding of interfacial processes is a prerequisite for developing advanced Li-ion battery (LIB) systems

Sn Anode for Li-ion Battery Systems

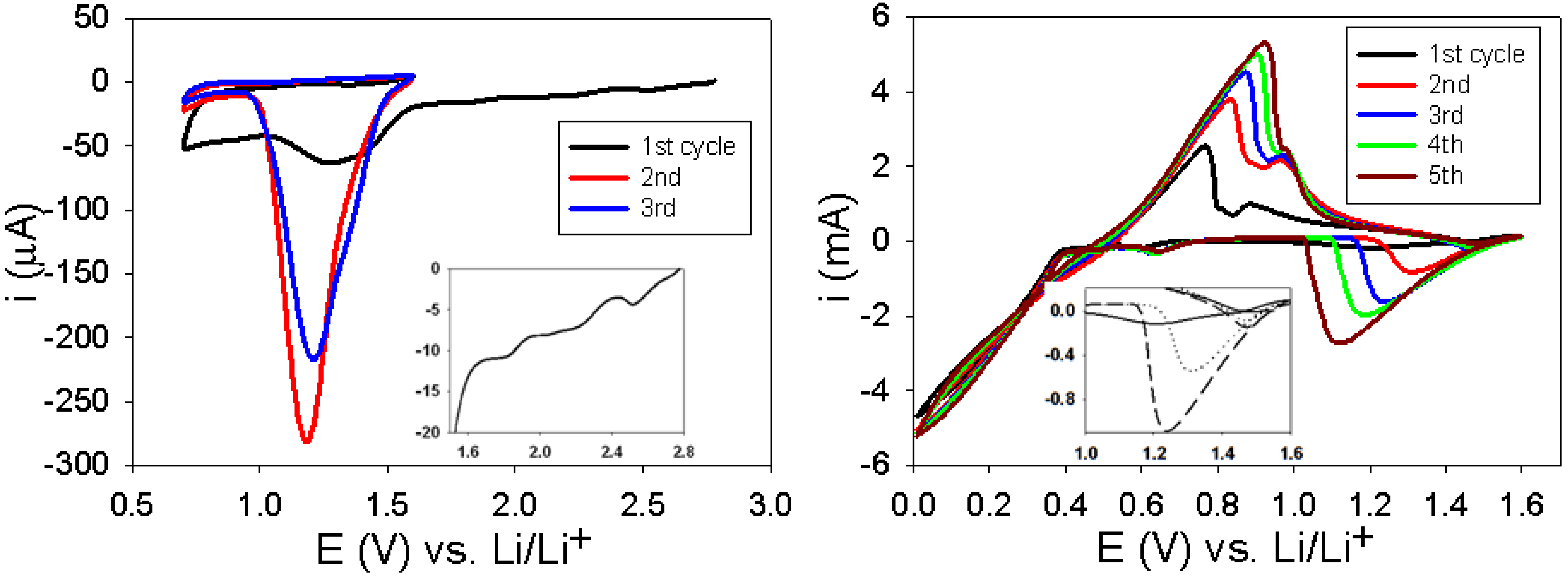

Sn-foil in 1M $LiPF_6$, EC:DEC (1:2)

- Irreversible electrolyte reduction peaks appear at 1.45 and 1.2 V
  - The peak at 1.45 V remains unchanged whereas the intensity of the peak at 1.2 V quadruples during the two following cycles.
- Large volumetric changes of Sn crystallites lead to Sn particle decrepitation and continuous regeneration of a fresh tin surface and SEI reformation

Assessment of Interfacial Processes at β-Sn Electrode

Experimental Approach

In situ AFM SEM *In situ* ellipsometry EDX

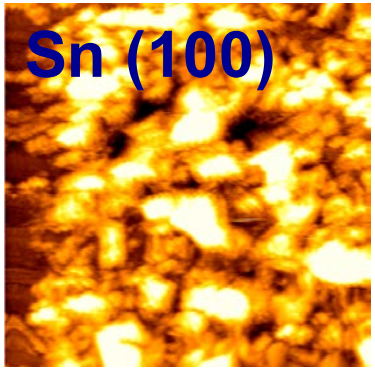

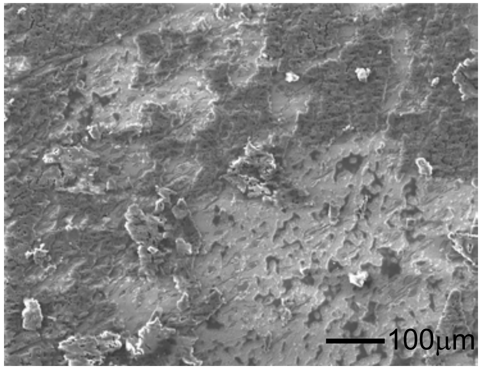

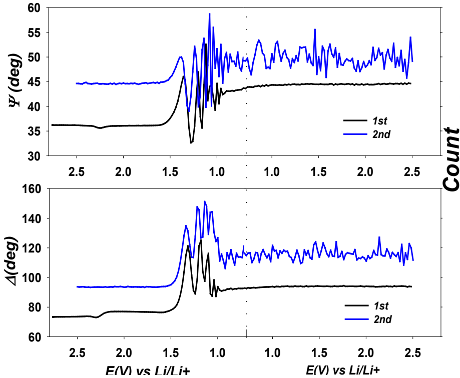

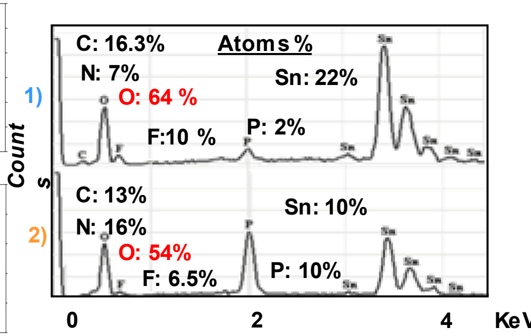

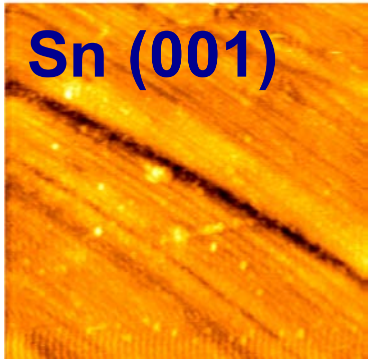

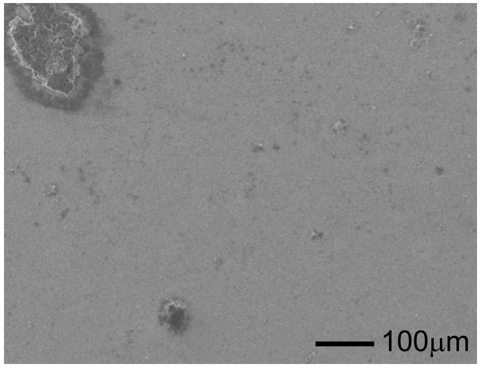

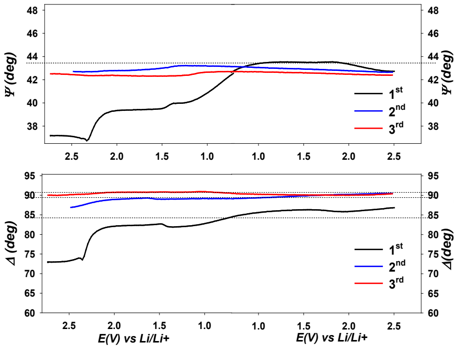

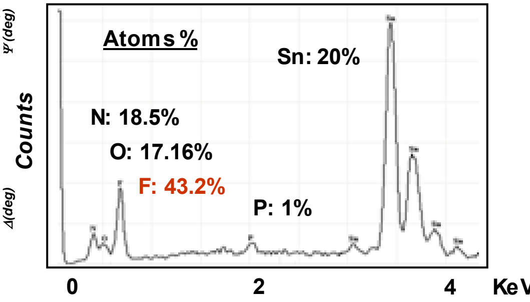

- Sn (001) electrode produces a very thin but effective SEI layer after one CV cycle
- Formation of an effective SEI layer is considerably delayed on the Sn (100) electrode. Continuous reformation of the SEI layer is very similar to the behavior of polycrystalline Sn.

Surface Structure of Sn (100) and Sn (001)

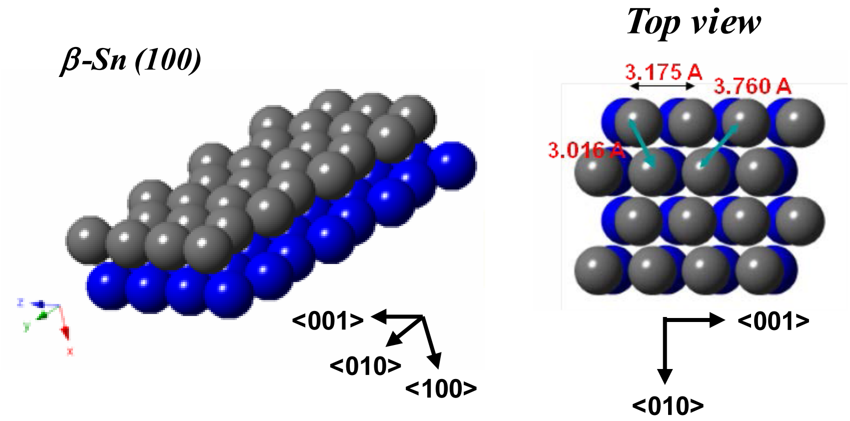

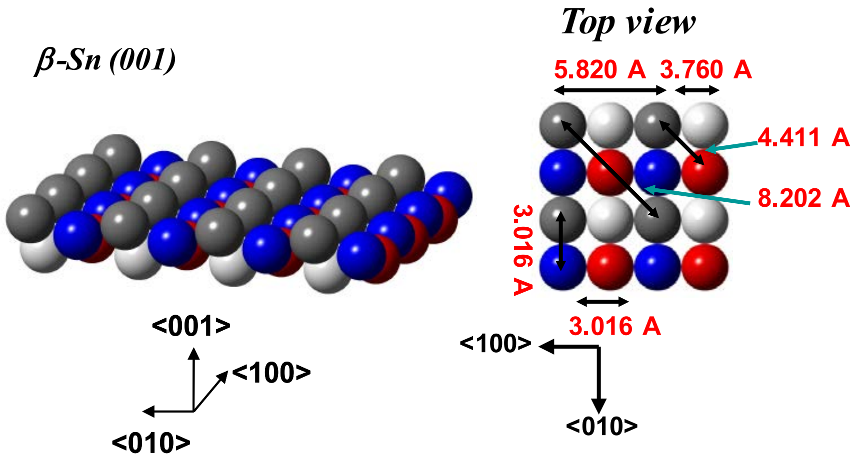

Surface atoms are densely packed and occupy **a single plane** that consist of Sn atoms with coordination number “**5**

Surface atoms occupy four distinct planes that consist of Sn atoms with coordination number “3” or “5.

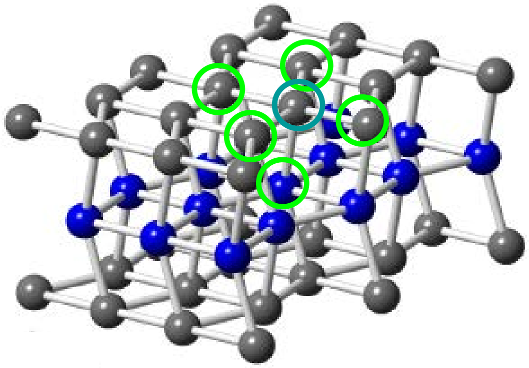

DFT calculation* and density of state plots:
(100): 0.02 eV/A^2
vs.
(001): 0.029 eV/A^2

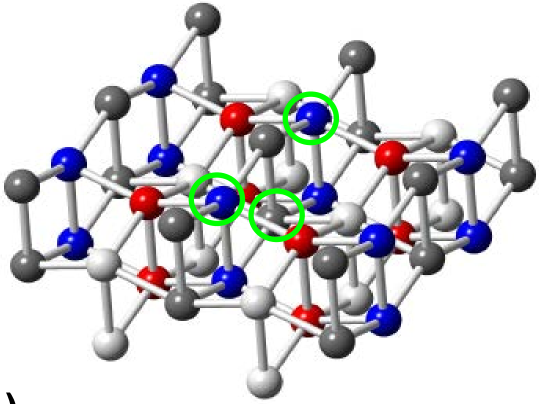

- **Surprisingly Sn (100) should be less reactive than Sn (001)**

→ *Competitive reduction processes on (100) delays the formation of an effective SEI layer*

- **Surface groups on Sn (001) possibly promote passivation processes**

* Courtesy of Kristin Persson

Reactivity of β-Sn Single Crystals

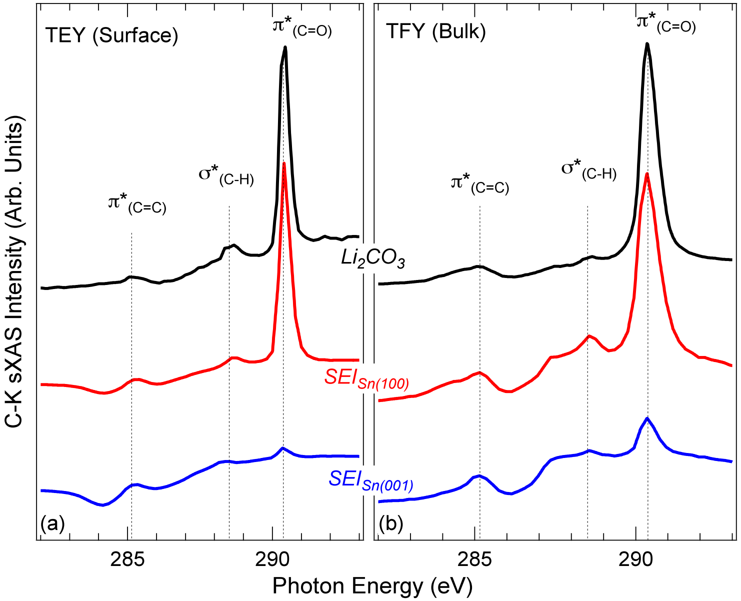

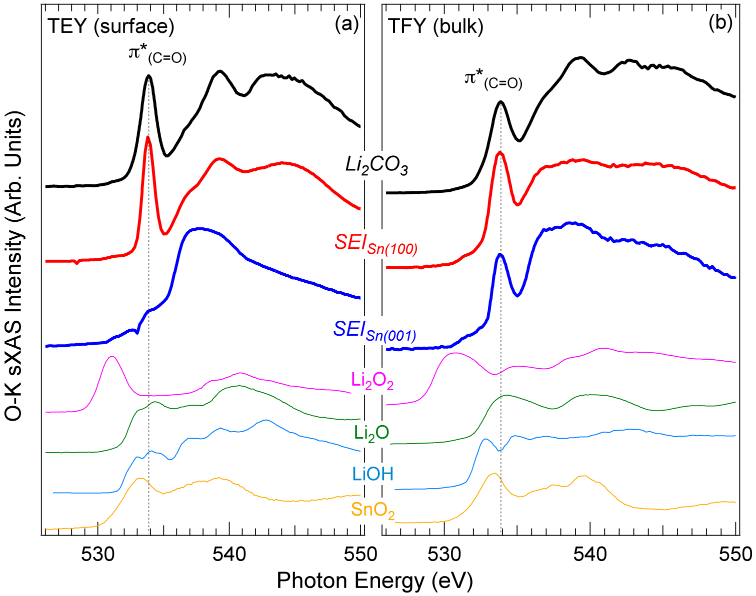

Material	(100)	(001)
Single crystal β-Sn	0.35	0.45
SnO_2	1.15	1.76
Hydrogen covered SnO_2	3.08	5.01

Calculated Surface Energies (J/m^2) of Sn-based single crystals with different surface orientations. Calculations for SnO_2 and hydrogen covered SnO_2 was made on tetragonal Sn with O connected to the non-coordinated surface Sn atoms

Qiao, R., Lucas, I. T., Karim, A., Syzdek, J., Liu, X., Chen, W., Persson, K., Kostecki, R. and Yang, W. (2014), Distinct Solid-Electrolyte-Interphases on Sn (100) and (001) Electrodes Studied by Soft X-Ray Spectroscopy. Advanced Materials Interfaces. doi: 10.1002/admi.201300115

Reactivity of Pure β-Sn Single Crystals

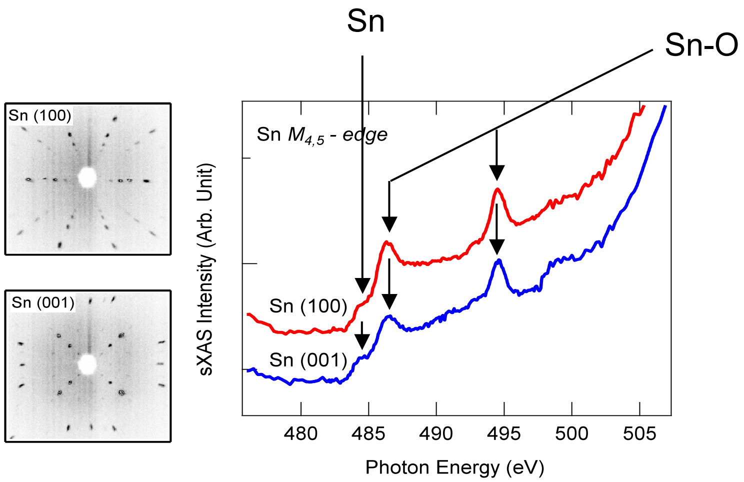

Sn *M*-edge soft XAS of pristine Sn electrode

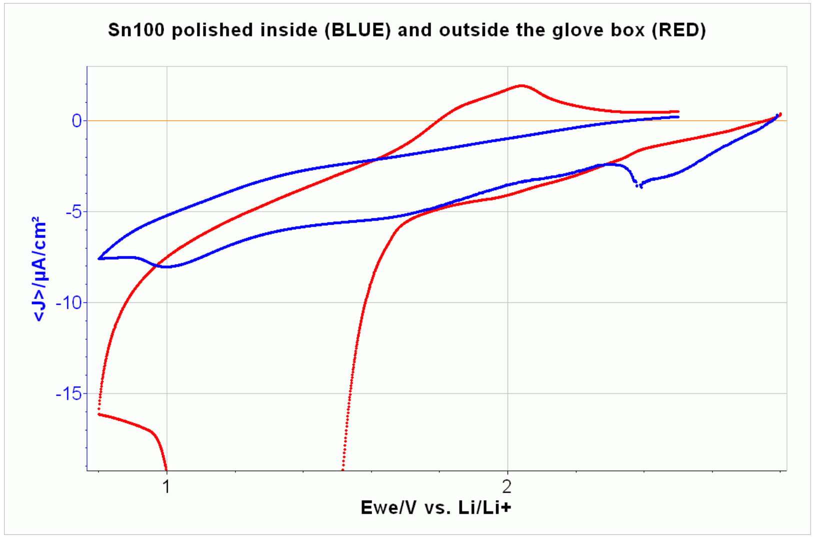
Sn100 polished inside (BLUE) and outside the glove box (RED)

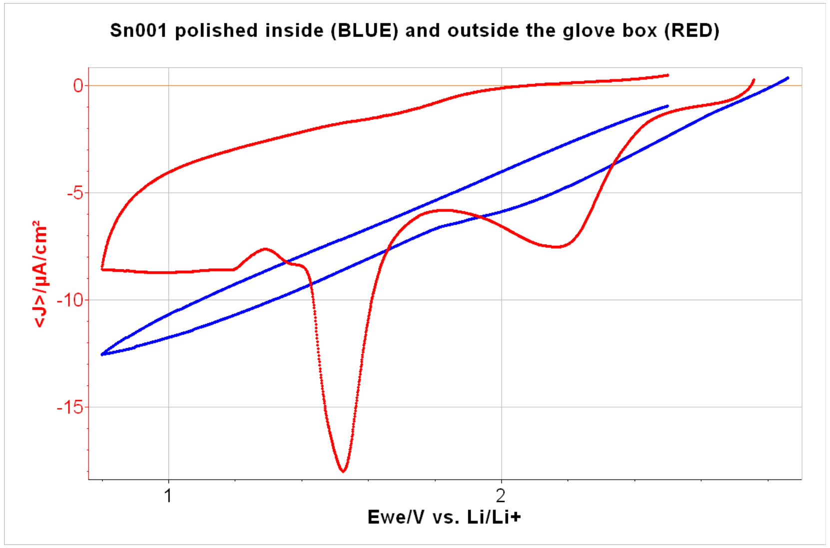
Sn001 polished inside (BLUE) and outside the glove box (RED)

- Sn dissolves appreciable amounts of oxygen and quickly passivates with an oxide film
- Presence of surface oxide changes significantly Sn reactivity toward organic carbonate electrolytes!

Reactivity of Pure β-Sn Single Crystals

Sn100

Sn001

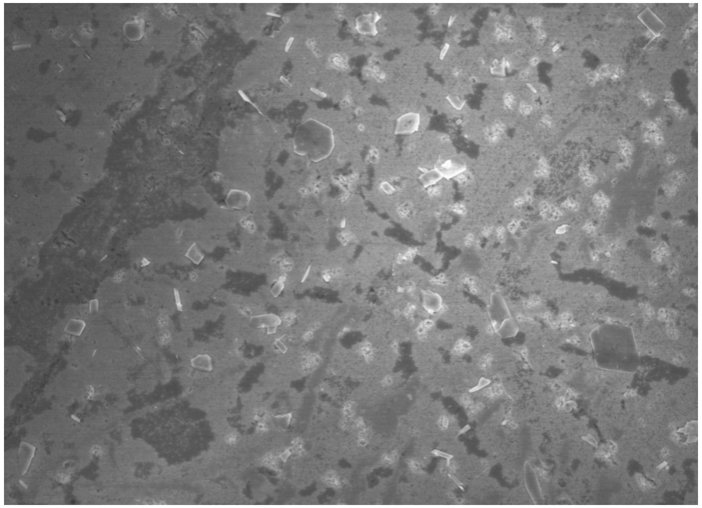

LiF
On both facets

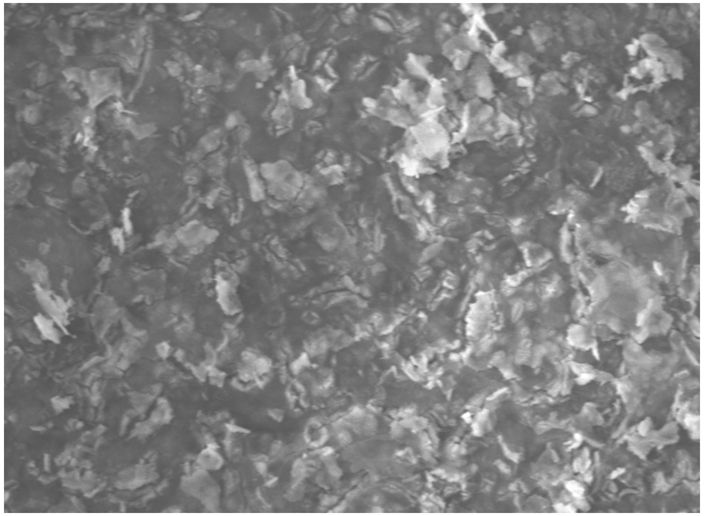

Surface (SEI) chemistry is strongly affected by the presence of surface oxides

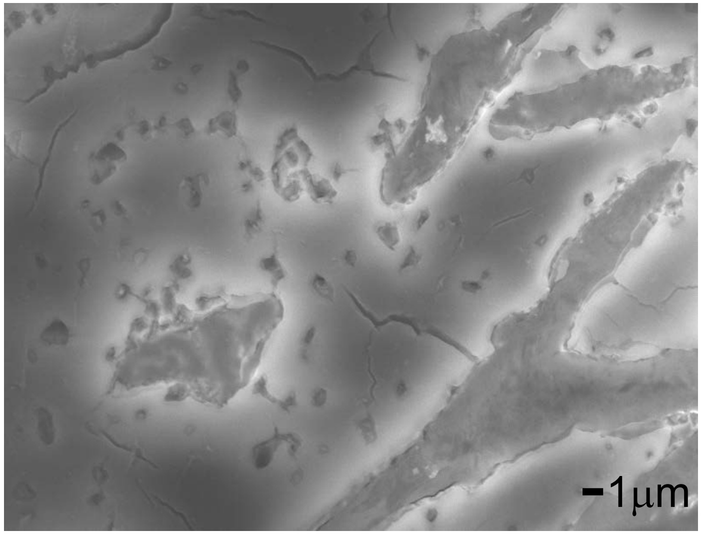

LiF →

← Li_2CO_3

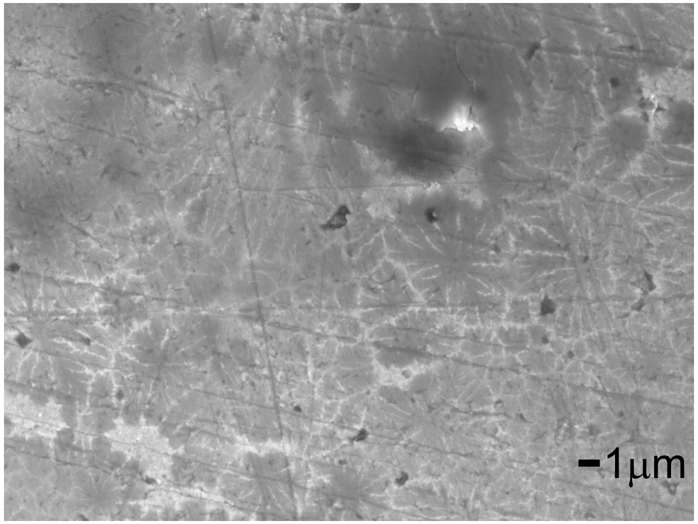

Near-Field IR Spectroscopy: Imaging of SEI on a Polycrystalline Sn Electrode

Topography

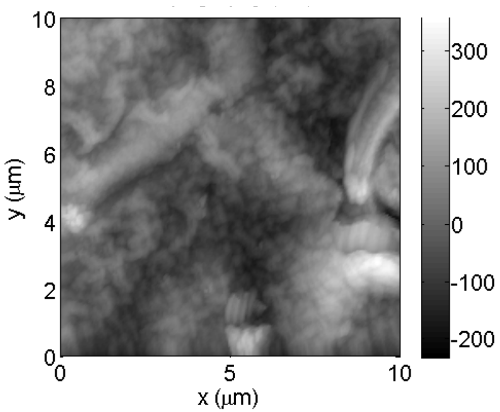

Near-Field IR Images at Single Wavelengths

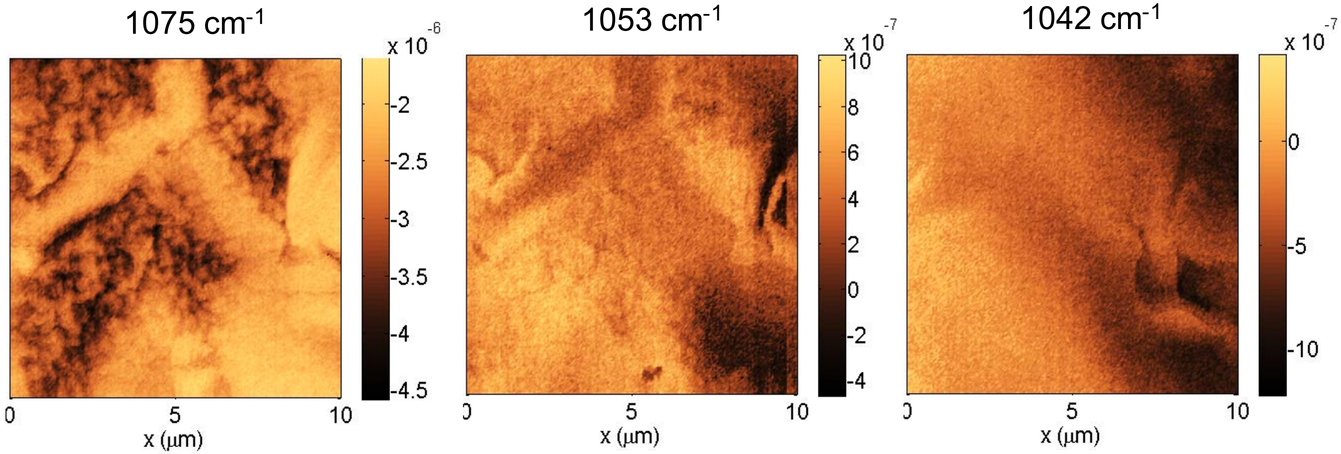
1075 cm^{-1}

1053 cm^{-1}

1042 cm^{-1}

- Topography and IR chemical composition images of the same area were recorded at a variety of wavelengths at 20 nm lateral resolution
  - Mapping indicates relative IR absorption due to dipole-phonon coupling
  - Chemical contrast images correlate to specific features in topography-> possibility to measure chemical distribution
- Changes in N-F signal intensity and contrast as the function of the incident IR wavelength represents variations of SEI layer chemical composition

Nano-spectroscopic Characterization of Battery Materials with Synchrotron Infrared Radiation

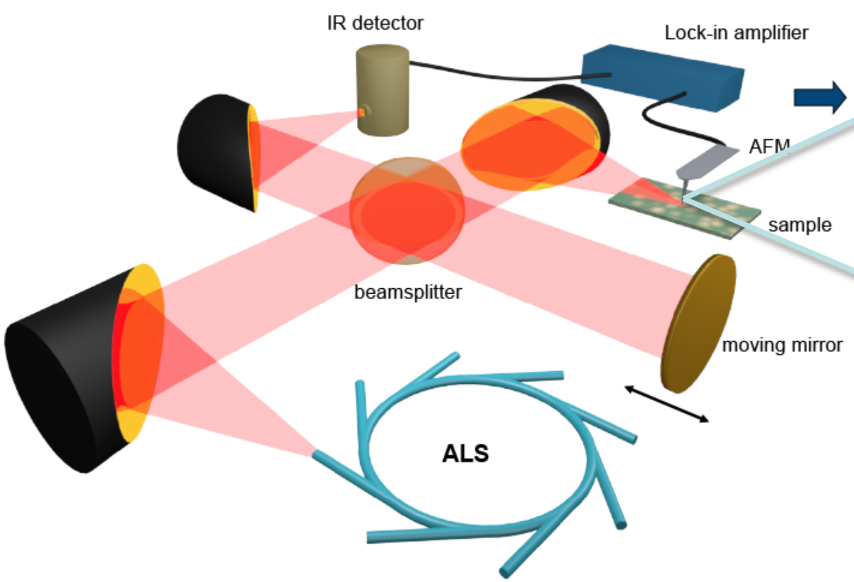

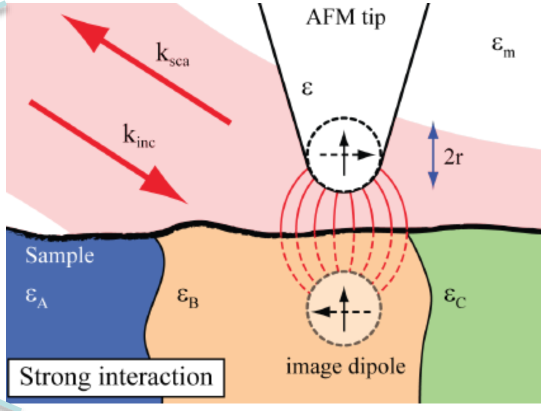

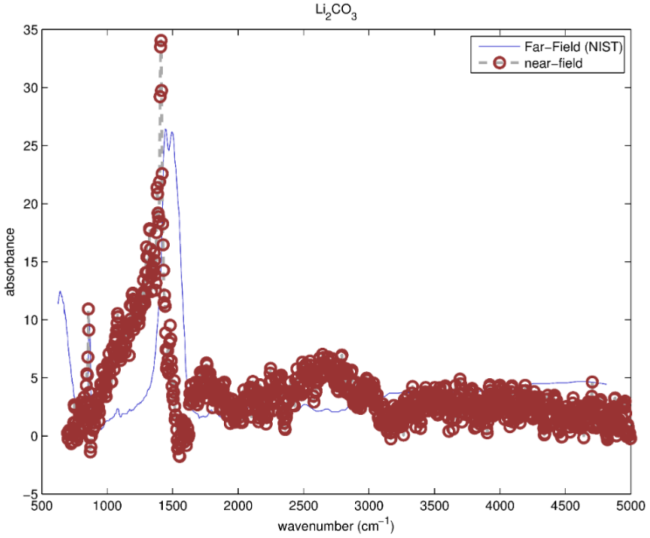

- Nanometer spatial resolution
- Wavelength independent
- Soft and hard matter
- Amplitude and phase of optical field

IR nano-spectroscopy allows identification of very similar phases with unprecedented 3D sensitivity in gentle beam conditions at <20 nm resolution

Near-Field nano-FTIR Spectroscopy of Sn SEI Layer with Synchrotron IR Source (ALS)

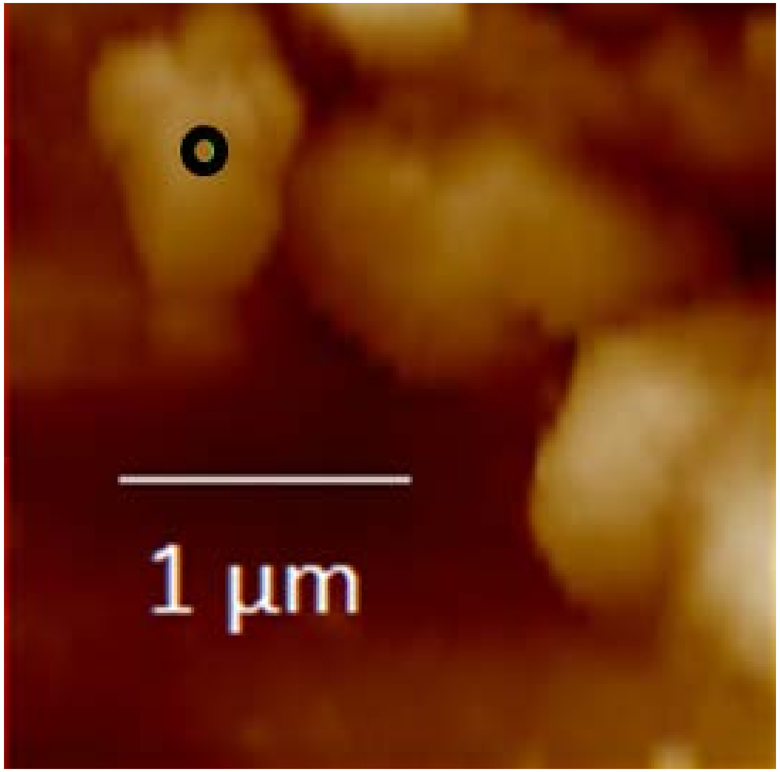

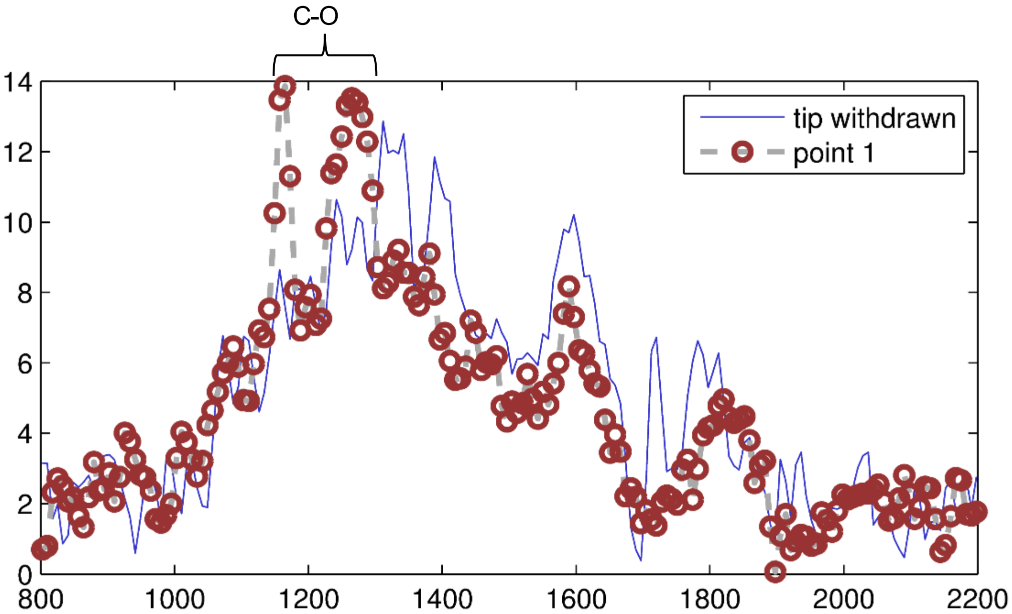

- Spectra taken at deeply subwavelength (20 nm) points chosen according to AFM topography
- Sn SEI nano-FTIR spectrum displays peaks at wavenumbers that correspond to -C-O, -C=0 indicating carbonates/organic compounds.

Near-Field IR Imaging of SEI Layer on Sn
Spatial Distribution of Li_2CO_3/$(CH_2OCO_2Li)_2$

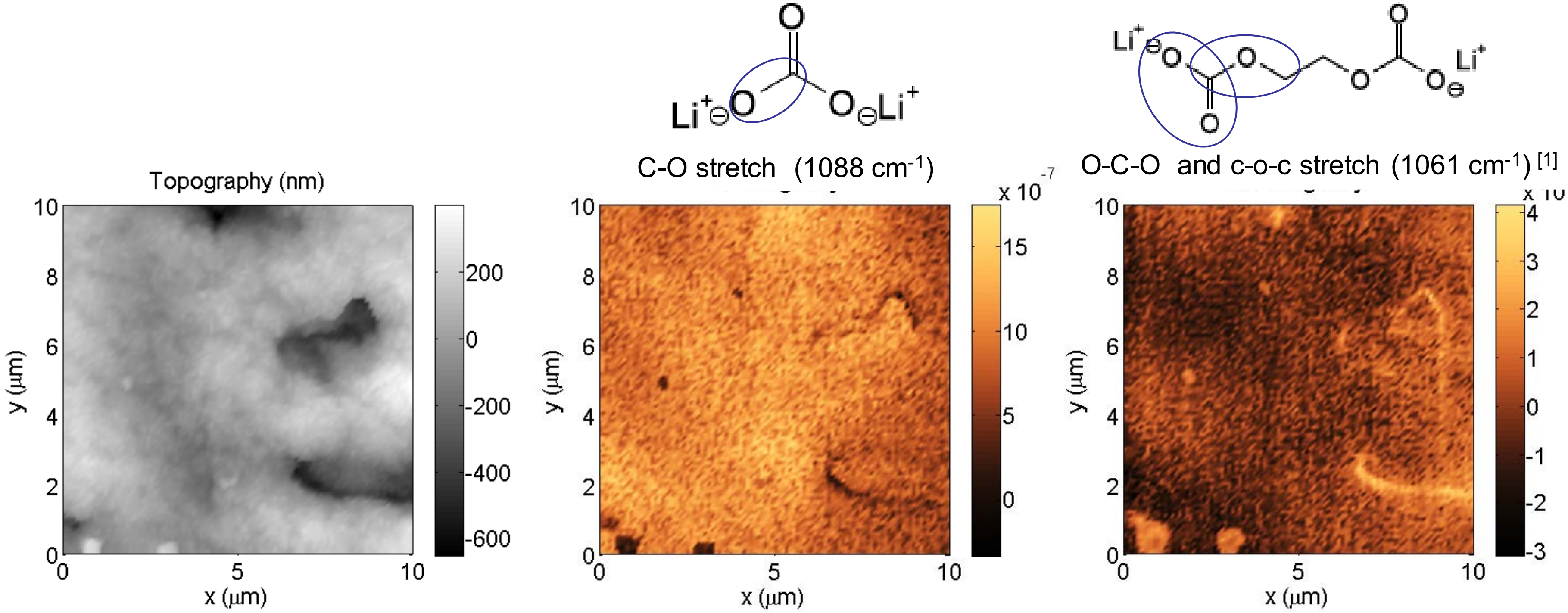

- Mapping second-harmonic signal at resonance indicates possible distribution of Li_2CO_3 in SEI layer on tin
- $(CH_2OCO_2Li)_2$ distributed at edges of pits in SEI Inverse contrast compared to Li_2CO_3

Zhuang et al. J. Phys. Chem. B 2005, 109, 17567-17573

Summary II

- *In situ* and *ex situ* studies revealed that the nature and kinetics of interfacial processes strongly dependent on the electrode surface structure.
  - The composition and effectiveness of the SEI layer on β-Sn single crystal electrodes in EC-DEC $LiPF_6$ electrolytes varies strongly with the Sn crystal surface orientation. The irreversible capacity observed on polycrystalline β-Sn strongly depends on the surface distribution of theses crystal domains with different reactivity.
  - Presence of residual SnO_2 strongly affects Sn surface reactivity, chemistry of the SEI and the irreversible capacity.
  - Oxygen-free Sn surfaces produces compact and stable SEI layers!
- Near-field FTIR spectra of the SEI layer are similar to far-field spectra for reference compounds. However, the SEI layer constituents are inhomogenously distributed across the electrode surface.
  - Spectra of real samples display nano-FTIR peaks associated with compounds thought to be in the SEI

A new class of emerging instrumental tools with an unprecedented analytical capabilities toward electrical energy materials and systems is still needed

"With this underpinning knowledge, wholly new concepts in materials design can be developed for producing materials that are
capable of storing higher energy densities and have long cycle lifetimes"

Future Work

- Apply novel far- and near-field optical multifunctional probes to obtain detailed insight into the dynamic behavior of molecules, atoms, and electrons at electrode/electrolyte interfaces of intermetallic anodes (Si) and high voltage Ni/Mn-based materials at a spatial resolution that corresponds to the size of basic chemical or structural building blocks.
- Unveil the structure and reactivity at hidden or buried interfaces and interphases that determine battery performance and failure modes.
- Develop and apply novel innovative experimental methodologies to study and understand the basic function and mechanism of operation of materials, composite electrodes, and molecular cross talk in Li-ion cells.
- Understand the mechanism of chemical "poisoning' of SEI by metal coordination complexes formed at the LMNO cathode. Identify underlying principles that govern charge and mass transport phenomena in the SEI layer using model systems and well-defined chemistry e.g., monomolecular films on intermetallic anodes.
- Cooperate with the BATT Task Groups "Intermetallic Anodes", "High-Voltage Cathodes" and industrial partners to investigate the effect of material structure, morphology on formation of the SEI layer.

Technical backup slides

Origins of Fluorescence in High-energy Li-ion Cells

Several organic aromatic compounds exhibit fluorescence in the visible range which intensity is directly correlated to their concentration[1].

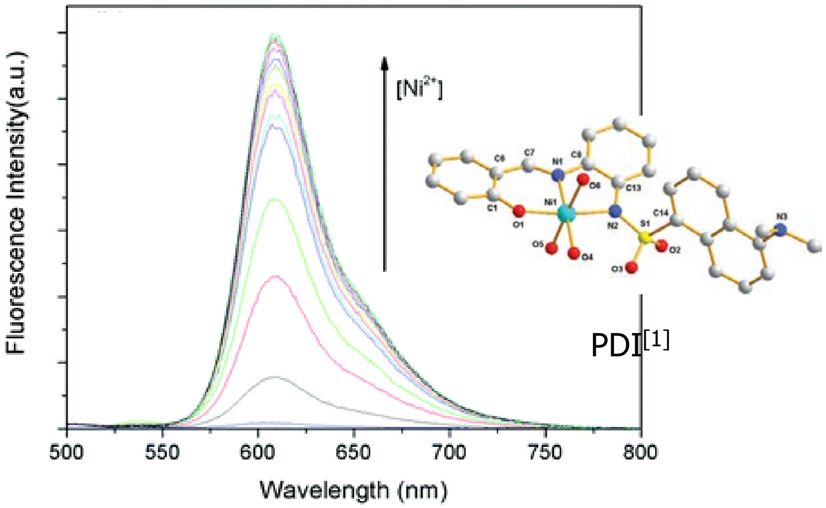

PDI[1]

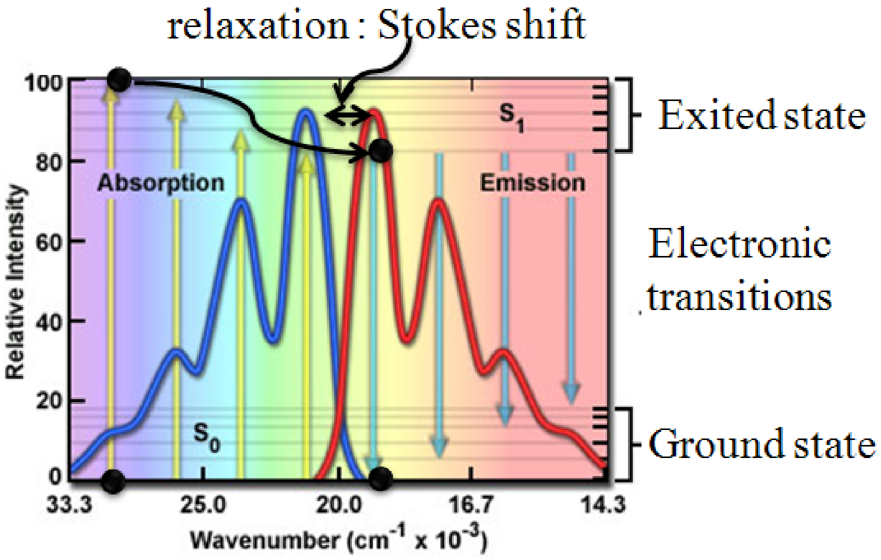

- Absorption and emission spectra that represent electronic transitions can be used to identify the structure and composition of the coordination complex molecule.
- Fluorescence allow a single molecule detection and provide information on dynamic processes on the nanosecond timescale

[1] H. Wang, D. Wang, Q. Wang, X. Li and C. A. Schalley, *Organic & Biomolecular Chemistry*, **8,** 1017 (2010)

Electronic Transitions in Octahedral Complexes

Based on the crystal field theory, d-d transitions with Ni^{2+} or Mn^{2+} and ligands with strength similar to water will lead to an absorption at 488 nm and a broad emission

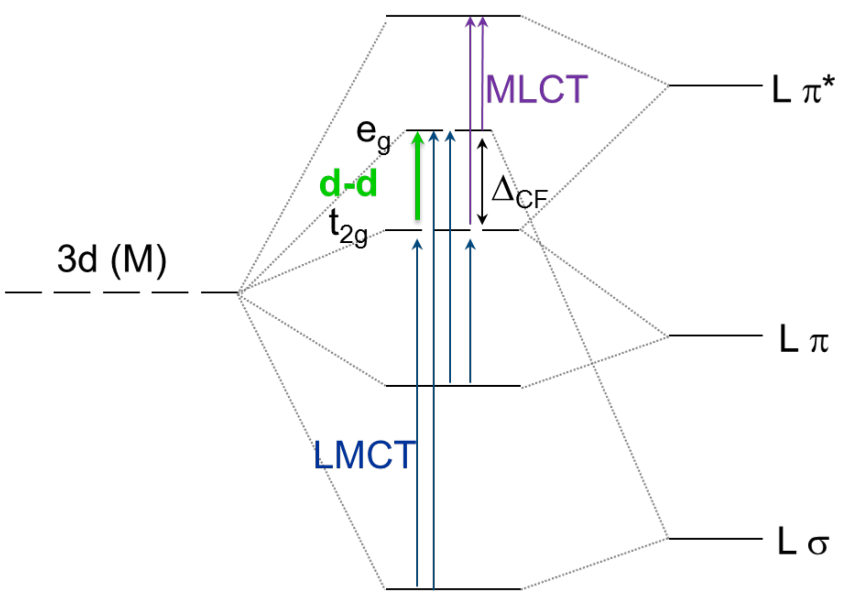

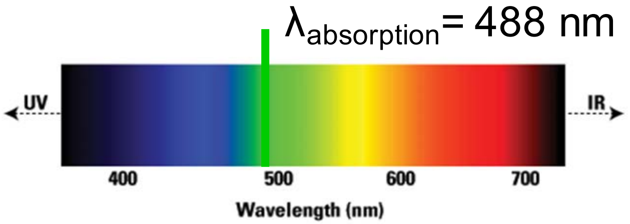

Transitions related to colored metal complexes are either d–d transitions or charge transfer

LMCT >> MLCT > | d-d

The energy splitting (Δ_{CF}) is correlated to the metal, its oxidation state and to the ligands nature

Co^{3+} > Co^{2+} > | Ni^{2+} > Mn^{2+}

CO > NO_2^- > | acac ≈ H_2O > OH^- > NO_3^- > I^-

Additional energy splitting are possible due to spin orbit effect

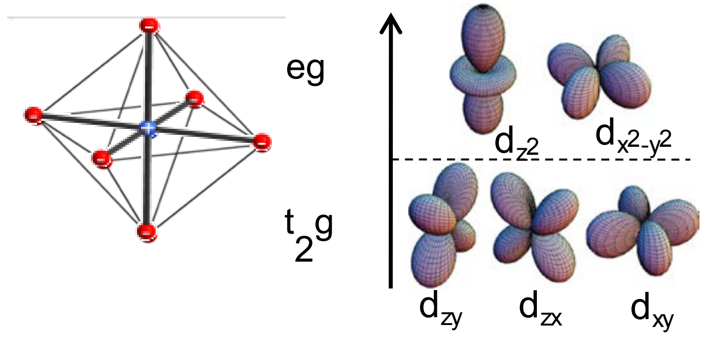

Y. Tokura, N. Nagasoa, Science, 2000, 288, 462 – 468

Near-Field Microscopy: Theoretical Background

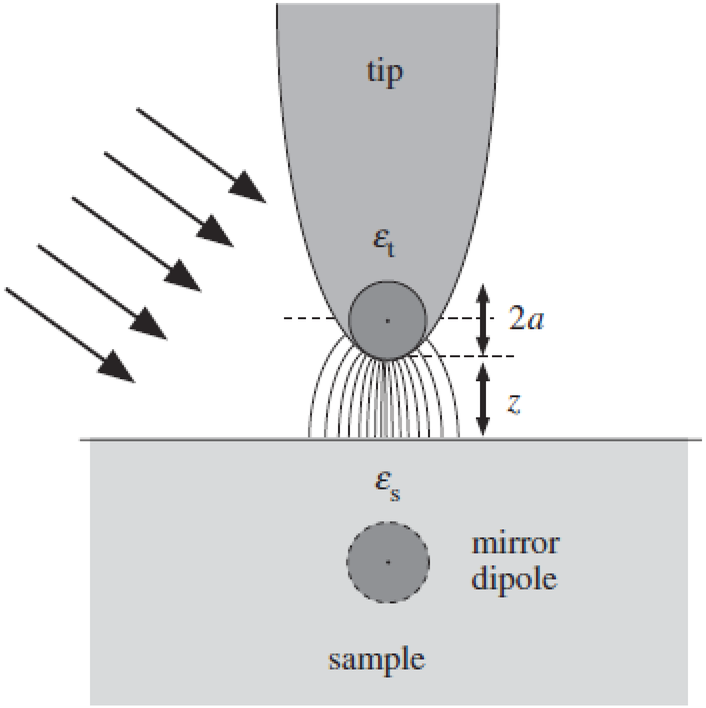

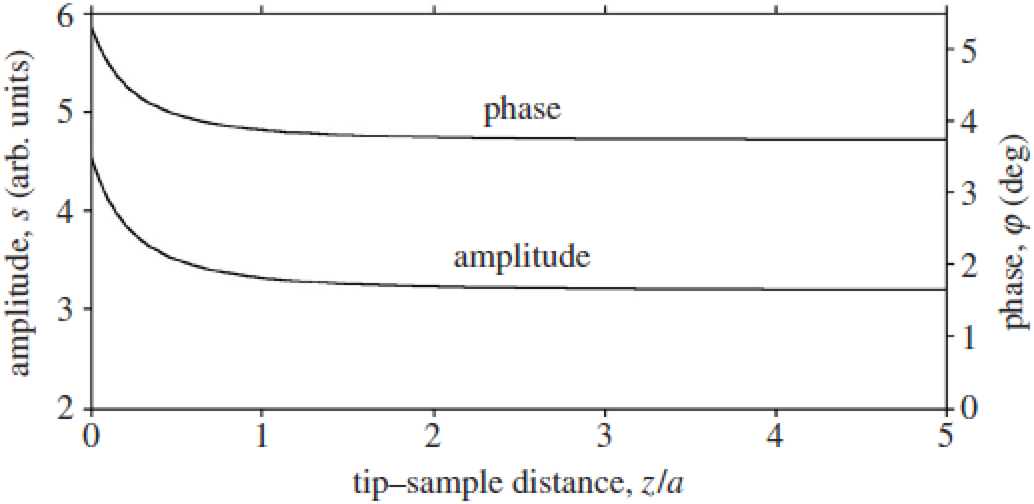

Keilmann, Hillebrand, Phil. Trans. Royal Society 362(1817):787–805 (2004)

$$\alpha = 4\pi a^3 \frac{\boxed{\varepsilon_t} - 1}{\boxed{\varepsilon_t} + 2}. \qquad \beta = \frac{\boxed{\varepsilon_s} - 1}{\boxed{\varepsilon_s} + 1} \qquad \alpha_{\text{eff}} = \frac{\alpha(1+\beta)}{1 - \alpha\beta/(16\pi(a + \boxed{z})^3)}.$$

- The nonlinear dependence $\alpha_{\text{eff}}(z)$ is used to eliminate unwanted ‘background’ scattering which generally dominates the detected signal.
- The focused laser beam illuminates a greater part of the tip shaft which typically extends 10µm from the cantilever, and also the sample.

From Dielectric Function to Near-Field Response

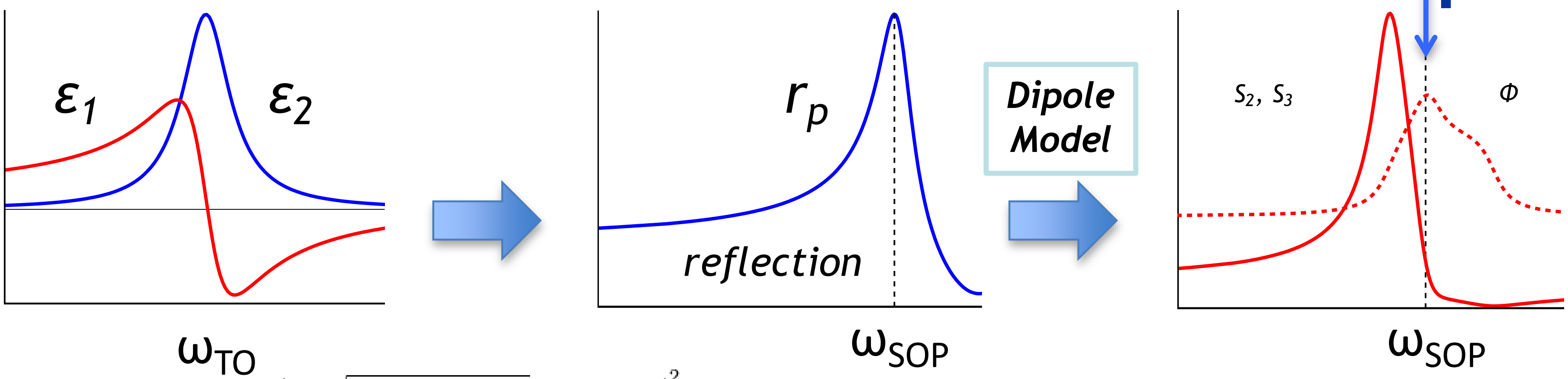

$$R_\mathrm{p} = \left|\frac{n_1\cos\theta_\mathrm{t} - n_2\cos\theta_\mathrm{i}}{n_1\cos\theta_\mathrm{t} + n_2\cos\theta_\mathrm{i}}\right|^2 = \left|\frac{n_1\sqrt{1-\left(\frac{n_1}{n_2}\sin\theta_\mathrm{i}\right)^2} - n_2\cos\theta_\mathrm{i}}{n_1\sqrt{1-\left(\frac{n_1}{n_2}\sin\theta_\mathrm{i}\right)^2} + n_2\cos\theta_\mathrm{i}}\right|^2$$

Fresnel equation for a single interface refraction

$$\begin{aligned}
d\lambda_\mathrm{nf}(z) &= dE_s \frac{d\lambda_\mathrm{nf}(z)}{dE_s} \\
&= dE_t \left(\mathcal{P}_{t\to s} \left.\frac{dE_{scat}}{dE_{inc}}\right|_s \mathcal{P}_{s\to t} \frac{d\lambda_{nf}(z)}{dE_{scat}} \right) \\
&= dQ_t \left(\frac{dE_t}{dQ_t} \mathcal{P}_{t\to s} \left.\frac{dE_{scat}}{dE_{inc}}\right|_s \mathcal{P}_{s\to t} \frac{d\lambda_{nf}(z)}{dE_{scat}} \right) \\
&= dQ_t \int_0^\infty dq \left(\frac{d}{dQ_t}\left(\frac{dE_{Q,t}}{dq}\right) \mathcal{P}_{t\to s}(q) \int_0^\infty dq' \left.\frac{dE_{scat,q'}}{dE_{inc,q}}\right|_s \mathcal{P}_{s\to t}(q') \frac{d\lambda_{nf,q'}(z)}{dE_{scat,q'}} \right) \\
&\equiv dQ_t \iint_0^\infty dq\, dq'\, \mathcal{G}(q)\, \mathcal{P}_{t\to s}(q)\, R(q,q')\, \mathcal{P}_{s\to t}(q')\, \Lambda(q',z)
\end{aligned}$$

Alex McLeod Swinton. PhD thesis, 2013

$$\alpha = 4\pi a^3 \frac{\varepsilon_\mathrm{t} - 1}{\varepsilon_\mathrm{t} + 2}, \qquad \beta = \frac{\varepsilon_\mathrm{s} - 1}{\varepsilon_\mathrm{s} + 1}$$

$$\alpha_\mathrm{eff} = \frac{\alpha(1+\beta)}{1 - \alpha\beta/(16\pi(a+z)^3)}.$$

a – tip radius
α – polarizability of the tip apex
ε_t – dielectric function of the tip
ε_s – dielectric function of the sample
β – dielectric surface response function of the sample
α_{eff} – effective polarizability of the coupled tip-sample system
z – tip-sample distance
$\varepsilon_{1,2}$ – Re and Im part of the dielectric function
ω_{TO} – transverse optical phonon frequency
ω_{SOP} – Surface optical phonon frequency
$S_{2,3}$ – Near field amplitude, 2nd, 3rd harmonic
Φ – optical field phase shift

[1] Keilmann, Hillebrand, Phil. Trans. Royal Society 362(1817):787–805 (2004)

Near-Field IR Microscopy

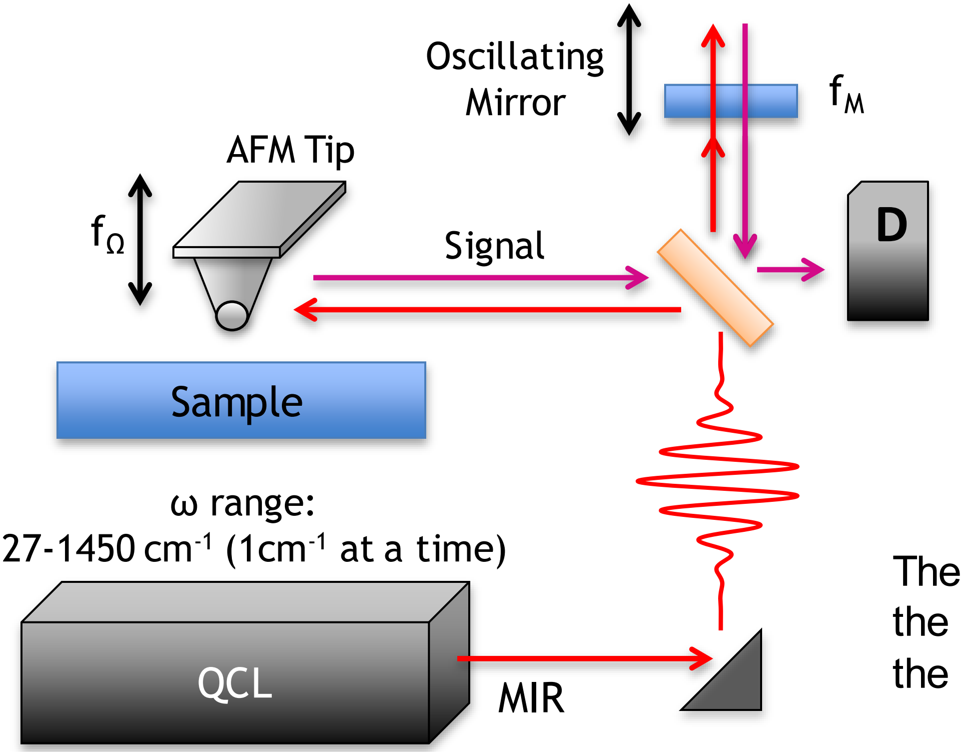

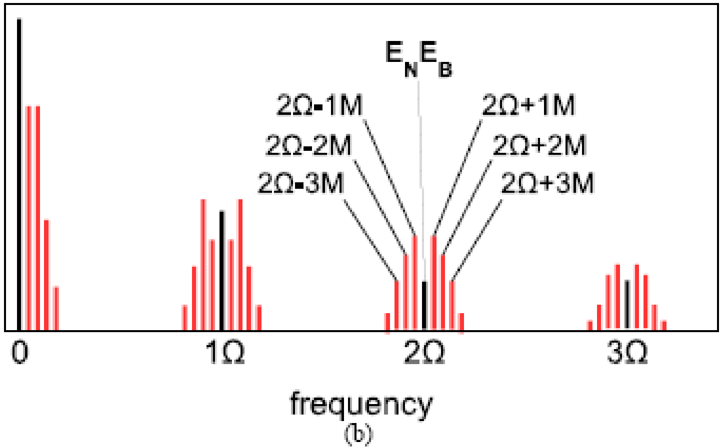

The demodulation of the detector output at a the side frequency $fn,m = n\Omega + mM$ provides the near-field signal amplitude and phase Om.

Laser beam focused on a vibrating mirror M (phase modulated reference beam at f_M = 300Hz) and on the oscillating AFM tip (f_Ω = 300KHz).

Background-free near field signal within an integration time of 6.5 ms (to 1.6 s) allowing fast raster scan imaging (~ 150 pixels / s).